JOURNAL OF CATALYSIS 142, 325–336 (1993)

Oxidative Coupling of Methane over a Li^+/MgO Catalyst Using N_2O as an Oxidant

HIROSHI YAMAMOTO, HON YUE CHU, MINGTING XU, CHUNLEI SHI, AND JACK H. LUNSFORD[1]

Department of Chemistry, Texas A&M University, College Station, Texas 77843

Received December 14, 1992; revised February 22, 1993

Nitrous oxide is an effective oxidant for the conversion of CH_4 to C_2H_4 and C_2H_6 over a Li^+/MgO catalyst, although the rate of oxygen incorporation into the lattice and the regeneration of the active centers is much slower with N_2O than with O_2. Thus, except at very low CH_4 partial pressures, the rate-limiting step is oxygen incorporation, rather than the activation of CH_4 at the surface. Carbon dioxide is a poison for the production of $CH_3\cdot$ radicals and for the conversion of CH_4. By extrapolation of the rate data, the rate of CH_4 reaction over the unpoisoned catalyst was determined, and the rate was shown to be first order with respect to N_2O. A kinetic model, based on competitive surface reactions, in addition to gas-phase reactions, adequately accounts for the conversion as a function of reagent concentrations and temperature, as well as the selectivity for ethane and ethylene. At comparable levels of conversion O_2 is a less selective oxidant than N_2O, not because of more gas-phase oxidation, but because of surface reactions involving reactive oxygen species. The presence of CH_4 significantly inhibits the decomposition of N_2O over the catalyst. It is suggested that CH_4 and N_2O are activated by a common intermediate (e.g., O^- ions) and that CH_4 reacts more rapidly with this species. © 1993 Academic Press, Inc.

INTRODUCTION

In most studies on the oxidative coupling of CH_4 to C_2H_6 and C_2H_4 (C_2 compounds), molecular oxygen has been used as the oxidant. Because the coupling reaction is a complex network of heterogeneous and homogeneous reactions, it is instructive to employ other oxidants, such as nitrous oxide. Otsuka and Nakajima (*1*) previously obtained kinetic data for the oxidative coupling reaction over Sm_2O_3, using N_2O as the oxidant. They observed that at a relatively low temperature for the oxidative coupling reaction (550°C) N_2O resulted in the formation of C_2H_6 with high selectivity, while complete oxidation occurred with O_2 as the oxidant. Moreover, N_2O decomposition was believed to be the rate-limiting step in the catalytic cycle. Hutchings *et al.* (*2, 3*) have also compared N_2O and O_2 as oxidants. They found that over a Li^+/MgO catalyst the conversion of CH_4 was an order of magnitude greater with O_2 than with N_2O when the oxidants were compared at the same pressure, but when the conditions were adjusted such that the conversions were the same, the C_2 selectivities were greater with N_2O (85% C_2 selectivity with N_2O and 50% C_2 selectivity with O_2). Additional results obtained with N_2O as an oxidant have been reviewed by Hutchings and Scurrell (*4*).

The origin of CO_2 during the oxidative coupling of CH_4 is still a matter of conjecture; however, it is clear that certain important gas phase reactions occur with O_2, but not with N_2O. For example, the reaction

$$CH_3\cdot + O_2 \rightarrow CH_2O + OH\cdot \qquad (1)$$

supplies hydroxyl radicals which are known to be chain carriers in the combustion of hydrocarbons. By contrast, the analogous reaction with N_2O,

$$CH_3\cdot + N_2O \rightarrow CH_3O\cdot + N_2, \qquad (2)$$

does not form $OH\cdot$ radicals. But our previ-

[1] To whom correspondence should be addressed.

0021-9517/93 $5.00
Copyright © 1993 by Academic Press, Inc.
All rights of reproduction in any form reserved.

ous attempts to model the heterogeneous-homogeneous coupling reaction over Li^+/MgO with O_2 as the oxidant suggested that gas phase reactions do not account for more than 10% of the CO_x at short residence times, at 700°C, and with low partial pressures of reagents (*5*). If this is indeed the case, then one must look for other explanations for the differences in selectivities. Molecular oxygen may form a different type of active site on the surface that is responsible for the complete oxidation of the hydrocarbons in the system. Such a site might be O_3^- ions, which are known to be formed at low temperatures by the reaction (*6*)

$$O_s^- + O_2 \rightarrow O_{3s}^-. \qquad (3)$$

Here, the subscript "s" refers to a surface species. In stoichiometric reactions ozonide ions were found to be much less selective than O^- ions in the dehydrogenation of alkanes over MgO (*7*).

As an oxidant for a kinetic study N_2O has a distinct advantage over O_2 with respect to the range of CH_4/O_2 ratios that can be explored. At CH_4/O_2 ratios ≤ 1, complete combustion begins to dominate, whereas, with N_2O as the oxidant large C_2 selectivities are observable under differential conditions, even at CH_4/N_2O ratios of 0.1. As a consequence the entire range of rate-limiting steps may be examined, from oxygen incorporation in the catalyst at one extreme to C–H bond breaking at the other extreme. Since nonselective secondary reactions involving the oxidant are less likely to occur, it also is possible to study the rate of methyl radical formation over a much broader range of oxidant partial pressures with N_2O than with O_2. This investigation was carried out in an effort to explore further the mechanism of the oxidative coupling reaction over Li^+/MgO catalysts. It was of particular interest to determine the origin of the apparent activation energies that are obtained under truly rate-limiting conditions.

EXPERIMENTAL

The Li^+/MgO catalyst was prepared by heating an aqueous slurry of Li_2CO_3 and MgO (Aldrich) to 100°C for several hours and then evaporating the water. The dry sample was sieved to 20–45 mesh and calcined in air at 750°C for 10 h. The amount of lithium loaded on the MgO was 4.1 wt%. After calcination the surface area of the catalyst was 2.7 m^2/g. For comparison, a low-surface-area MgO catalyst was prepared by heating the high purity oxide at 930°C for 10 h in a sealed fused-quartz tube. The resulting material had a surface area of 8.5 m^2/g. In order to prevent excessive gas pressure, the tube with the catalyst was evacuated at elevated temperatures before sealing.

The kinetic studies were carried out in a plug-flow reactor constructed of fused quartz. The upper section of the reactor, which contained the catalyst, was 10 mm i.d., and the lower section was constructed of 1-mm-i.d. capillary tube. The smaller diameter allowed the products to pass rapidly out of the heated zone. A thermocouple was located at the level of the catalyst on the outside of the reactor. In a separate experiment, the temperature inside the catalyst bed was compared to that measured outside of the reactor, and it was found that the temperature difference was only 1°C.

All of the kinetic results were obtained under nearly differential conditions. The conversion of the limiting reagent was $\leq$ 20%. In these studies 0.731 g (0.79 cc) of Li^+/MgO or 0.269 (0.94 cc) of MgO catalyst was loaded between 1-mm-thick layers of quartz wool. Quartz chips were placed above the catalyst to aid in preheating the reactant gas and to minimize the free volume. A blank experiment was carried out with only quartz chips in the reactor, and it was found that with 40 kPa CH_4, 61 kPa N_2O, a flow rate of 50 ml/min, and at 680°C, the conversion of CH_4 and N_2O was only 0.1%.

The reactant gases were premixed before entering the reactor using mass flow controllers. The total flow rate was about 50 ml/min. Helium was used as a diluent to achieve a total pressure of 101 kPa. The purities of

the CH_4 and N_2O, both from Matheson, were 99.97 and 99.0%, respectively. Gas chromatography was used to analyze the product stream. Separation of the various components was achieved using molecular sieve and Porapak R columns.

The rate of CH_4 consumption generally was calculated from summation of the moles of products, taking into account the stoichiometric factors. At the larger conversion levels the amount of CH_4 converted also was determined by difference. In such cases the material balance, based on the carbon, was greater than 95%.

Methyl radical formation was obtained using the matrix-isolation electron spin resonance (MIESR) system that has been described previously (*8*). Briefly, radicals which exit a thin layer of catalyst enter a leak into a differentially pumped region. The radicals are frozen in an argon matrix on a sapphire rod maintained at 15 K, and, after a certain collection period, their ESR spectra are recorded. The total pressure in the region of the catalyst was ca. 0.1 kPa.

The kinetic isotope effect (KIE) was obtained from the isotopic distribution of H and D in the ethane product. The experiment was performed using a known mixture of CH_4/CD_4. The sensitivities and fragmentation patterns of pure methanes (CH_4 and CD_4) and ethane (C_2H_6 and C_2D_6) were first obtained using a GC/MS system at typical experimental conditions, and then the standard fragmentation pattern of CH_3CD_3 was calculated. The relative amounts of C_2H_6, CH_3CD_3, and C_2D_6 were calculated based on the mass spectra of the product ethane and the previously determined sensitivities and fragmentation patterns of these three materials. The KIE was then calculated using the relative amount of CH_3 and CD_3 in the ethanes. The error associated with the KIE obtained in this manner is estimated to be less than 5%.

RESULTS

Decomposition of N_2O

Many metal oxides are known to be effective catalysts for the decomposition of N_2O at elevated temperatures (*9*, *10*); therefore, it was of interest to explore briefly the properties of Li^+/MgO for this reaction. At a pressure of 40 kPa N_2O the conversion of N_2O was studied over the temperature range from 635 to 680°C. The conversion levels were found to be 5 and 15% at 635 to 680°C, respectively. From data obtained over this temperature range an E_a of 192 ± 8 kJ/mol was determined. Surprisingly, the addition of even 10 kPa CH_4 had a strong negative effect on the rate of N_2O reaction over the Li^+/MgO catalyst. Based on the amount of N_2 that appeared in the gas phase, the N_2O decomposition decreased to 1 and 2.5% at 635 and 680°C, respectively. When the CH_4 pressure was increased to 30 kPa, the effect on the N_2O reaction was essentially the same. As will be subsequently shown, the amount of O_2 in the gas phase was very small when CH_4 was present. The negative effect of CH_4 on the catalytic decomposition of N_2O is an advantage for this study, as the presence of relatively large amounts of O_2 would complicate the interpretation of the following results.

Kinetic Data for Oxidative Coupling

Conversion and selectivity data were obtained for the reaction of CH_4 with N_2O over the temperature range from 635 to 680°C. Selected data, obtained by varying the partial pressure of CH_4 from 5 kPa to 40 kPa, while keeping the partial pressure of N_2O constant at about 60 kPa, are shown in Table 1 and Fig. 1. As noted in Table 1, the C_{2+} selectivity was quite large (70 to 91%) even though the methane-to-oxidant ratio was considerably less than unity. With O_2 as the oxidant, even at a CH_4/O_2 ratio of 5.4 (see below), the C_{2+} selectivity was only 62% for 10.7% CH_4 conversion at 680°C. Because of the larger selectivity obtained with N_2O the absolute amount of CO_2 produced was small and the poisoning effect of CO_2 was less severe. The amount of O_2 that appeared as a product was negligible, therefore its role in the oxidation process (both heterogeneously and homogeneously) can be largely

TABLE 1

Effect of CH_4 Partial Pressure on the Catalytic Reaction over Li^+/MgO

CH_4/N_2O[a] (kPa)	CH_4 Conv. (%)	Selectivity (%)				CO_2[b] (kPa)	O_2[c] (kPa)
		C=C	C–C	C_3	CO_2		
4.3/59.4	21.2(21.3)[d]	40(15)	22(52)	7(0.6)	30(24)	0.28	0.01
8.9/60.1	14.2(14.9)	39(14)	29(60)	9(0.6)	22(19)	0.27	0.01
19.1/60.4	8.6(8.3)	37(11)	38(66)	11(0.5)	13(15)	0.22	0.00
38.1/59.6	4.7(4.3)	32(9)	49(69)	10(0.3)	9(14)	0.16	0.00

[a] Pressure of reactants, T = 680°C.
[b] The CO_2 in the system was derived from the reaction.
[c] The O_2 in the system was derived from the reaction.
[d] The numbers in parentheses were determined from the model (see text).

discounted. Similarly, the amount of CO formed was below the detection limits.

The rate of CH_4 conversion, as shown in Fig. 1, increased with increasing partial pressure of CH_4 up to about 10 kPa, but at higher partial pressures the reaction became almost zero order with respect to CH_4 pressure. The effect of CO_2 produced during the reaction will be subsequently discussed; however, at this point it is sufficient to note from the data of Table 1 that at 680°C the amount of CO_2 decreased from 0.28 to 0.16 kPa as the CH_4 partial pressure was increased from 4.3 to 38.1 kPa. At a constant level of CO_2 poisoning the conversion, for example at 4.3 kPa in Fig. 1, would be increased about 30%. The net result is that after factoring out the effect of varying CO_2 partial pressures the reaction would become zero order with respect to CH_4 at even lower partial pressures than indicated in Fig. 1.

The results obtained while keeping the partial pressure of CH_4 constant at ca. 9.5 kPa and varying the pressure of N_2O are summarized in Table 2 and Fig. 2. Again, the selectivity for C_{2+} products was large (≥ 80%), and almost no O_2 was formed. From Fig. 2 it appears that the orders with respect to CH_4 and N_2O are similar; however, the consequences of CO_2 poisoning

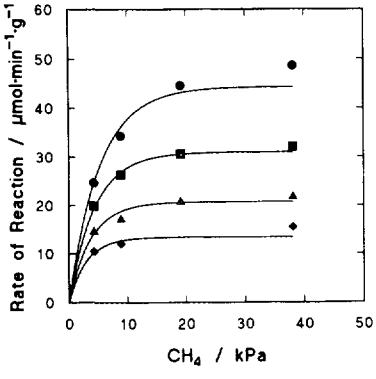

FIG. 1. Dependence of CH_4 consumption over Li^+/MgO on CH_4 pressure, while keeping the N_2O pressure constant at ca. 60 kPa: (◆) 635°C, (▲) 650°C, (■) 665°C, and (●) 680°C. The solid lines were calculated using the model.

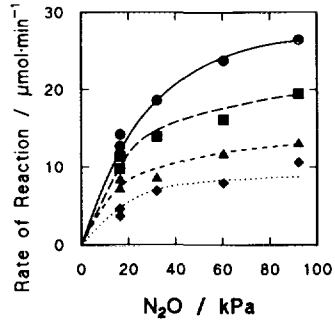

FIG. 2. Dependence of CH_4 consumption over Li^+/MgO on N_2O pressure, while keeping the CH_4 pressure constant at ca. 10 kPa: (◆) 635°C, (▲) 650°C, (■) 665°C, and (●) 680°C.

TABLE 2

Effect of N_2O Partial Pressure on the Catalytic Reaction over Li^+/MgO

CH_4/N_2O^a (kPa)	CH_4 Conv. (%)	Selectivity (%)					CO_2^b (kPa)	O_2^c (kPa)
		C=C	C-C	C_3	CO_2	CO		
9.6/16/4	4.9	32	52	6	9	0	0.04	0.01
9.8/16.5	5.4	32	51	8	9	0	0.05	
9.2/32.1	7.5	36	44	9	12	0	0.08	0.01
8.7/60.4	10.4	36	37	11	16	0	0.15	0.02
9.2/92.2	10.7	36	35	9	20	0	0.20	0.03

[a] Pressure of reactants, T = 680°C.

[b] The CO_2 in the system was derived from the reaction.

[c] The O_2 in the system was derived from the reaction.

are very different for the two cases. Although the *total* pressure of CO_2 remained small, a fivefold increase in CO_2 pressure occurred as the N_2O pressure was increased from 16.4 kPa to 92.2 kPa. This means that the intrinsic (i.e., unpoisoned) rates of reaction may be significantly greater than those shown in Fig. 2, particularly at the greater N_2O pressures.

To determine quantitatively the effect of CO_2 poisoning a series of experiments was carried out in which CO_2 was added to the gas stream. One set of results is shown in Fig. 3, where it is evident that even small partial pressures of CO_2 have a remarkable poisoning effect. In this figure the pressure of CO_2 corresponds to that produced during the reaction plus any that was added to the reagents. The points at the lowest CO_2 level were obtained without the addition of any CO_2.

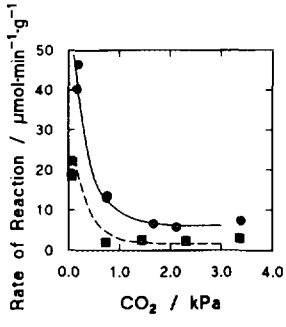

FIG. 3. The effect of CO_2 on the rate of CH_4 conversion to C_{2+} products over Li^+/MgO: $P(CH_4)$ = 30 kPa, $P(N_2O)$ = 70 kPa; (■) 650°C and (●) 680°C.

Obviously one would like to know the intrinsic activity of the unpoisoned catalyst in order to obtain the true order of reaction with respect to N_2O. In a previous kinetic study, with O_2 as the oxidant, Ross and coworkers (*11*) factored out the effect of CO_2 by adding a rather large amount of CO_2 to the system, thus the reaction became pseudo zero order with respect to CO_2. We have chosen to extrapolate the rate data to zero CO_2 pressure, using the rate equation

$$R = \frac{k \cdot f[P(CH_4) \cdot P(N_2O)]}{1 + K \cdot P(CO_2)}. \qquad (4)$$

This is the classic equation that one would obtain for a Rideal mechanism in which one of the products is a poison (*12*). At constant CH_4 and N_2O pressures the inverse of Eq. (4) yields

$$\frac{1}{R} = A + B \cdot P(CO_2). \qquad (5)$$

Indeed, a plot of $1/R$ versus CO_2 pressure yields a linear relationship (Fig. 4) and from the ordinate intercept the unpoisoned rate can be determined. The rate of reaction is equated to the rate of C_{2+} formation in order to avoid the errors that would be introduced

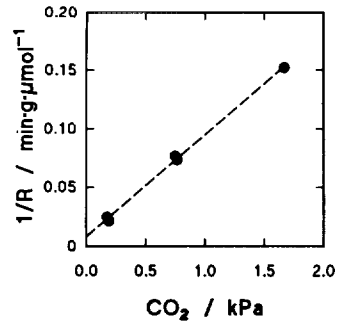

FIG. 4. Inverse rate of CH_4 conversion to C_{2+} products as a function of CO_2 partial pressure: $P(CH_4)$ = 30 kPa, $P(N_2O)$ = 70 kPa; T = 680°C.

by determining the small amount of CO_2 that was formed during reaction in the presence of a large amount of added CO_2. The error introduced by equating the rates is small as the C_{2+} selectivity was large.

The poisoning experiments were carried out under four sets of conditions, and the results are shown in Fig. 5. Based on the

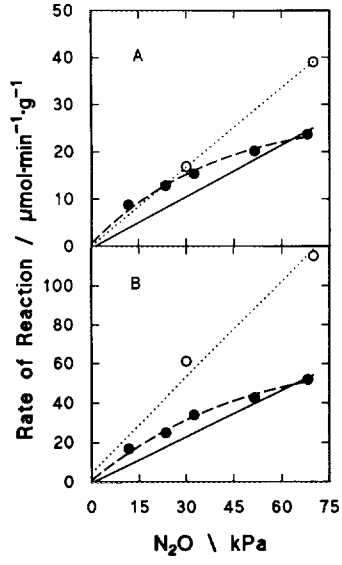

FIG. 5. Comparison of uncorrected (●) and corrected (○) rates for the conversion of CH_4 as a function of N_2O pressure. The corrected values were obtained by extrapolation of the rates to zero partial pressure of CO_2 at (A) 650°C and (B) 680°C. The solid lines were calculated using the model.

TABLE 3

KIE Results for Methane Oxidation over Li^+/MgO

Methane[a] (kPa)	KIE	
	Measured	Calculated[b]
2	1.6	1.5
20	1.1	1.1

[a] $P(N_2O)$ = 60 kPa, T = 680°C.
[b] Determined from the model (see text).

corrected rates it appears that the reaction is first order with respect to N_2O. The zero-order behavior with respect to CH_4 and first-order behavior with respect to N_2O suggest that oxygen incorporation into the lattice is the rate-limiting step in the mechanism. This is supported by a measure KIE near unity for the oxidation of methane with N_2O at 700°C (*13*). The KIEs were determined for CH_4-to-N_2O ratios of 1 : 3 and 1 : 8 at a total pressure of 760 Torr (no diluent). The range of the KIE measurements has been extended to more closely match the conditions of this experiment, and the results are shown in Table 3. Clearly, if the CH_4 pressure is sufficiently reduced (<2kPa), the breaking of the C-H bond becomes rate limiting.

From the results of Figs. 1 and 2 the activation energies reported in Table 4 were

TABLE 4

Activation Energy for CH_4 Oxidation over Li^+/MgO

CH_4/N_2O (kPa)	E_a (kJ/mol)	CO_2[a] (kPa)
9.2/32.1	170.8 ± 6.7	0.02–0.08
8.7/60.4	175.0 ± 4.2	0.04–0.15
9.2/92.2	158.2 ± 10.8	0.05–0.20
4.3/59.4	139.0 ± 7.5	0.08–0.28
8.9/60.1	157.4 ± 5.0	0.07–0.27
19.1/60.4	182.9 ± 2.5	0.08–0.22
38.1/59.6	187.9 ± 9.6	0.05–0.16

[a] The CO_2 in the system was derived from the reaction.

TABLE 5

Comparison of O_2 and N_2O as Oxidants for the Oxidative Coupling of CH_4

Oxidant	Temp. (°C)	CH_4 Conv.[a] (%)	Selectivity (%)					CO_2[b] (kPa)	O_2[c] (kPa)
			C=C	C–C	C_3	CO_2	CO		
O_2	635	3.0	7	22	1	46	25	0.42	4.62
O_2	646	3.9	10	24	1	44	21	0.53	4.36
O_2	665	7.1	16	37	2	34	11	0.76	3.76
O_2	680	10.7	22	36	4	32	6	1.06	3.07
N_2O	635	2.2	16	63	12	9	0	0.05	0.01
N_2O	650	3.1	23	59	10	9	0	0.08	0.01
N_2O	665	4.8	29	50	11	9	0	0.12	0.01
N_2O	680	6.8	35	44	11	10	0	0.19	0.01

[a] Reaction conditions: $P(CH_4)$ = 30 kPa, $P(O_2)$ = 5.6 kPa, and $P(N_2O)$ = 68 kPa.
[b] The CO_2 in the system was derived from the reaction.
[c] The O_2 remaining in the system after being consumed by reaction.

determined. Over the range for which oxygen incorporation was rate limiting, the E_a was approximately 167 ± 8 kJ/mol; only at the lowest CH_4 partial pressure did the E_a decrease to 138 ± 8 kJ/mol. One should keep in mind that CO_2 poisoning also has an effect on E_a, although the effect may be different on the steeper part of the CO_2 adsorption isotherm (see Fig. 3), which is the case with N_2O, than on the flatter part of the isotherm, which is applicable with O_2.

Comparison of N_2O and O_2 as Oxidants

In this study an attempt was made to compare N_2O and O_2 as oxidants at a nearly equal level of CH_4 conversion. This was achieved by measuring the CH_4 conversion level at an arbitrary set of N_2O and CH_4 pressures, and then substituting O_2 for N_2O. The O_2 pressure was adjusted such that the CH_4 conversions were similar at 646–650°C. The results, as shown in Table 5, may be summarized as follows: (i) comparable CH_4 conversions were achieved at a much lower partial pressure of O_2, (ii) the C_{2+} selectivity was greater with N_2O as the oxidant, (iii) a considerable amount of C_3 product was found with N_2O, and (iv) CO was detected only in the presence of O_2.

Comparison of Li^+/MgO and MgO as Catalysts

It has previously been reported that with O_2 as an oxidant pure MgO is a rather poor catalyst for the coupling reaction, both with respect to activity and selectivity (*14*). From the results of Table 6, it is evident that with N_2O as the oxidant MgO is also a nonselective catalyst, but the conversion was actually greater over the MgO. This implies that the poor selectivity of MgO is an inrinsic property of the material and is not related to the oxidant. With respect to the activity, one should note that the surface area of MgO was about three times that of the Li^+/MgO catalyst, therefore the specific activity of MgO is somewhat less than that of the Li^+/MgO catalyst.

MIESR Results

Methyl radical formation was observed over the Li^+/MgO catalyst both at small and large CH_4/N_2O ratios. The Arrhenius plots, shown in Fig. 6, reveal that the rate of production of $CH_3\cdot$ radicals increases with N_2O partial pressure. Previously it was reported that the $CH_3\cdot$ radical production rate increased almost linearly with respect to N_2O pressure up to a CH_4/N_2O ratio of unity, and at larger N_2O pressures the rate did not increase substantially (*13*). At a CH_4/N_2O ratio of 0.29, a KIE of 1.9 ± 0.2 was observed, whereas at a CH_4/N_2O ratio of 44, a KIE of 1.2 ± 0.2 was determined. These results are consistent with a change in the rate limiting step from C–H bond breaking to

TABLE 6

Comparison of Performance of Li^+/MgO and MgO Catalysts

Catalyst	CH_4 conv.[a] (%)	Selectivity (%)					CO_2[c] (kPa)	O_2[d] (kPa)
		C=C	C–C	C_3	CO_2	CO		
MgO[a]	4.6	5	9	1	76	10	1.01	0.08
Li/MgO[b]	2.6	20	60	11	8	0	0.06	0.01

[a] Reaction conditions: $P(CH_4)$ = 29 kPa, $P(N_2O)$ = 50 kPa; T = 650°C.
[b] Surface area = 8.5 m^2/g.
[c] Surface area = 2.7 m^2/g.
[d] The CO_2 in the system was derived from the reaction.
[e] The O_2 in the system was derived from the reaction.

oxygen incorporation as the CH_4/N_2O ratio increased. The change in E_a at 700°C from 75 ± 16 to 134 ± 8 kJ/mol as the CH_4/N_2O ratio increased also is consistent with the change in the rate-limiting step. Apparently, when the temperature becomes <600°C, the rate-limiting step changes at the large CH_4/N_2O ratios, and it becomes the same as at the small CH_4/N_2O ratios; namely, C–H bond breaking. The E_a associated with this rate-limiting step is 134 ± 8 kJ/mol. It is important to note that these E_a values were obtained under catalytic conditions, but at very low CO_2 partial pressures. As pointed out previously, the rate limiting step may be a function of the total pressure, as well as the CH_4/N_2O ratio and the temperature.

When CO_2 was substituted for Ar as the matrix-forming gas, there was a dramatic decrease in the production of $CH_3\cdot$ radicals, and the E_a increased by about 84 kJ/mol. A similar phenomenon was observed with O_2 as the oxidant (*15*). It follows from Eq. (4) that if $K \cdot P(CO_2) \gg 1$, $E_a = E + \lambda$, where λ is the heat of adsorption (or reaction) of CO_2. From the results of Fig. 6, one may conclude that λ = 84 kJ/mol, as was previously deduced with O_2 as the oxidant.

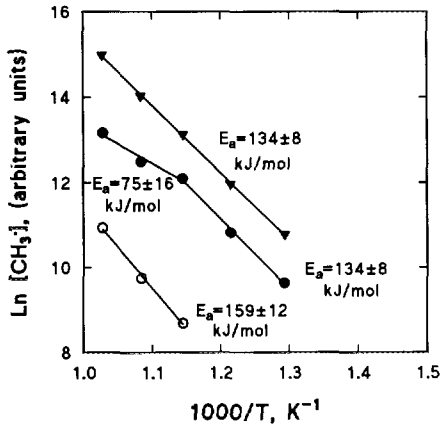

FIG. 6. Arrhenius plots for $CH_3\cdot$ radical formation: (▼) CH_4/N_2O = 1.1/3.8 ml min^{-1}, (●) $Ar/CH_4/N_2O$ = 3.8/1.1/0/025 ml min^{-1}, and (○) $CO_2/CH_4/N_2O$ = 3.8/1.1/0.025 ml min^{-1} at STP.

DISCUSSION

The mechanism first proposed by Ito *et al.* (*16*) for the oxidative coupling of CH_4 over Li^+/MgO catalysts may be modified to include N_2O as the oxidant,

$$CH_4 + O_s^- \rightarrow CH_3\cdot + OH_s^- \quad (6)$$

$$2OH_s^- \rightarrow H_2O + O_s^{2-} + \square \quad (7)$$

$$O_s^{2-} + \square + N_2O \rightarrow 2O_s^- + N_2 \quad (8)$$

$$2O_s^- \rightarrow O_s^{2-} + \square + \frac{1}{2}O_2, \quad (9)$$

where $\square$ is an oxide ion vacancy. An analogous set of reactions could be written with O_2^{2-} ions as the centers responsible for the activation of CH_4. If one assumes that reaction (8) is rate limiting, then the rate law

would be first order with respect to N_2O and zero order with respect to CH_4, as was observed over most of the range of conditions in the conventional catalytic experiments. In such a case the apparent activation energy of 75 ± 17 kJ/mol for $CH_3\cdot$ radical formation might be equivalent to the true activation energy for reaction (8). However, N_2O and CH_4 also may compete for the same active center, (see below) which would result in a more complex relationship for E_a. This phenomenon may explain the difference between E_a values of 167 ± 8 and 75 ± 17 kJ/mol obtained in the conventional mode and in the MIESR system, with both being carried out under conditions at which reaction (8) is rate limiting. Carbon dioxide poisoning also may contribute to this difference.

It is tempting to equate the E_a's of 138 ± 8 and 134 ± 8 kJ/mol obtained in the conventional reactor and the MIESR system, respectively, under conditions such that C–H bond breaking was rate limiting. The E_a obtained in the conventional reactor may have been subject to small effects of CO_2 poisoning. Nevertheless, assuming that such a comparison can be made, the value of 134 kJ/mol is not the activation energy for the C–H bond breaking step alone, but rather it is a linear combination of energies for several steps in the catalytic cycle.

In order to understand the negative effect of CH_4 on N_2O decomposition additional reactions should be included in the mechanism, for example, by adding the reactions

$$N_2O + O_s^- \rightarrow O_{2s}^- + N_2 \qquad (10)$$

$$N_2O + O_{2s}^- \rightarrow O_{3s}^- + N_2 \qquad (11)$$

$$O_{3s}^- \rightarrow O_2 + O_s^-. \qquad (12)$$

Here it becomes evident that CH_4 and N_2O may compete for the same O_s^- center via reactions (6) and (10). Thus, the presence of CH_4 would decrease the rate of N_2O decomposition. Apparently the rate of reaction (6) is considerably greater than that of reaction (10), as indicated by the strong negative effect of CH_4 on N_2O decomposition. As a consequence very little O_2 is produced via reaction (12), and also the overall consumption of CH_4 is first order, not zero or negative order with respect to N_2O. Unlike CO_2, N_2O serves both to produce and to remove active centers.

There is no direct evidence for reaction 10; however, reaction (11) was previously studied on MgO, and it was found to occur at $T \geq 100°C$ (*17*). Reaction (12) was also demonstrated when N_2O, and presumably a small amount of O_2, were removed at 25°C from a MgO sample that had O_{3s}^- ions (*17*). The mechanism for N_2O decomposition via reactions (8)–(12) avoids the problem of electron transfer from an insultor or p-type oxide to N_2O that is inherent in the mechanisms of Dell *et al.* (*9*) and Winter (*10*).

The kinetic model that was previously developed to study the heterogeneous-homogeneous reactions during oxidative coupling with O_2 as the oxidant (*13*) has been extended to include N_2O. The original 156 gas-phase reactions were included, as well as the additional reactions shown in Table 7. The reactions of N_2O with several important intermediates were included, in addition to reactions involving C_3 molecules. Qualitatively, the enhanced formation of C_3 products can be attributed to the competitive reactions

$$C_2H_5\cdot + O_2 \rightarrow C_2H_4 + HO_2\cdot \qquad (13)$$

and

$$CH_3\cdot + C_2H_5\cdot \rightarrow C_3H_8. \qquad (14)$$

If molecular oxygen is present, reaction (13) is an efficient means of converting ethyl radicals to ethylene, but in its absence reaction (14) becomes competitive with the unimolecular decomposition of ethyl radicals.

In the model the rate constants for the heterogeneous reactions (6)–(9) were treated as adjustable parameters, and reactions (10)–(12) were not included. The calculated results using $k_6 = 2.53 \times 10^{-15}$ $e^{-500/T}$ $cm^3 \cdot molecule^{-1} \cdot s^{-1}$, $k_7 = 2.00 \times 10^{-5}$ $e^{-0/T}$ $cm^3 \cdot molecule^{-1} \cdot s^{-1}$, $k_8 = 4.42 \times$

TABLE 7

Gas-Phase Reactions in the Heterogeneous–Homogeneous Model Rate constants $k = AT^n \exp[-E_a/RT]$, in units of mol · cm^{-3} · s^{-1}

Reaction	log(A)	n	E_a/R	Reference
$H + N_2O = NH + NO$	14.80	0	14594	(18)
$H + N_2O = OH + N_2$	13.88	0	7599	(18)
$O + N_2O = NO + NO$	13.65	0	12128	(18)
$O + N_2O = N_2 + O_2$	13.65	0	12128	(18)
$OH + N_2O = HO_2 + N_2$	8.38	0	0	(18)
$CH_3 + N_2O = CH_3O + N_2$	14.72	0	14276	(18)
$CH_4 + C_3H_5 = CH_3 + C_3H_6$	11.69	0	11258	(18)
$CH_4 + n\text{-}C_3H_7 = CH_3 + C_3H_8$	−1.62	4.02	5470	(19)
$CH_4 + i\text{-}C_3H_7 = CH_3 + C_3H_8$	−3.14	4.40	5440	(19)
$CH_3 + C_2H_4 = n\text{-}C_3H_7$	11.52	0	3877	(18)
$CH_3 + C_2H_5 = C_3H_8$	14.69	−0.5	0	(18)
$CH_3 + C_2H_2 = C_3H_5$	11.78	0	3877	(18)
$CH_3 + C_2H_3 = C_3H_6$	13.00	0	0	(20)
$CH_3 + C_3H_8 = CH_4 + n\text{-}C_3H_7$	12.34	0	6054	(18)
$CH_3 + C_3H_8 = CH_4 + i\text{-}C_3H_7$	12.08	0	5183	(18)
$CH_3 + C_3H_6 = CH_4 + C_3H_5$	10.64	0	3789	(18)
$n\text{-}C_3H_7 + O_2 = HO_2 + C_3H_6$	12.00	0	2530	(21)
$i\text{-}C_3H_7 + O_2 = HO_2 + C_3H_6$	12.00	0	1503	(21)
$n\text{-}C_3H_7 = CH_3 + C_2H_4$	38.27	0	16718	(18)
$n\text{-}C_3H_7 = C_3H_6 + H$	37.78	0	18763	(18)
$i\text{-}C_3H_7 = CH_3 + C_2H_4$	35.78	0	20567	(18)
$i\text{-}C_3H_7 = C_3H_6 + H$	38.08	0	19485	(18)
$n\text{-}C_3H_7 + H_2 = H + C_3H_8$	12.42	0	7448	(18)
$i\text{-}C_3H_7 + H_2 = H + C_3H_8$	12.40	0	8047	(22)
$n\text{-}C_3H_7 + H = CH_3 + C_2H_5$	13.03	0	0	(18)
$n\text{-}C_3H_7 + H = C_3H_8$	13.40	0	0	(19)
$i\text{-}C_3H_7 + H = C_3H_8$	13.30	0	0	(21)
$C_3H_6 + OH = CH_2O + C_2H_5$	12.90	0	0	(23)
$C_3H_6 + OH = H_2O + C_3H_5$	12.88	0	0	(18)
$C_3H_6 + H = H_2 + C_3H_5$	11.81	0	2237	(18)
$C_3H_5 + H = C_3H_6$	13.30	0	0	(24)

$10^9\ e^{-23,600/T}\ s^{-1}$, and $k_9 = 4.82 \times 10^{-13}\ e^{-0/T}$ are shown in Figs. 1 and 5, and the selectivities are given in Table 1. For computational purposes, reaction (8) was replaced by

$$N_2O \rightarrow N_2 + O_s^- . \qquad (8')$$

The activation energies for k_6 and k_8 were 4.1 and 196.2 kJ/mol, respectively. By suitably adjusting the preexponential factor an equally good fit to the data of Fig. 1 could be achieved upon increasing the E_a for k_6 to 40 kJ/mol; however, the fit was not nearly as good in the region of low CH_4 pressure when E_a's of 80 or 120 kJ/mol were used in the model. The model accurately predicts the functional relationships between the rate of CH_4 conversion and the partial pressures of CH_4 or N_2O, as well as the temperature effects. No assumptions are necessary concerning the rate-limiting step. The set of rate constants used to fit the data probably are not unique. The extrapolated rates in Fig. 5 were greater than the calculated rates because the model did not include CO_2 poisoning effects. When all gas-phase reactions were deleted from the model except the coupling of $CH_3\cdot$ radicals, the CH_4 conversion at 680°C, 8.9 kPa CH_4 and 60 kPa N_2O de-

creased from 15.0 to 11.9%. Thus, radical reactions in the gas phase result in only 3% more CH_4 conversion. The model also accurately predicts the change in the rate-limiting step as indicated by the KIEs (Table 3).

As shown in Table 1, the calculated selectivities for the combined C_2 products and CO_2 were in good agreement with those found experimentally. This agreement is surprising as the model did not include secondary reactions between the intermediates or stable products and the catalyst. We conclude, therefore, that CO_2 is formed primarily from the oxidation of C_2's in the gas phase, in contrast to the case with O_2 as the oxidant at these temperatures. Here it should be noted that the model does include the heterogeneous conversion of CO to CO_2. In contrast to the agreement in overall C_2 selectivity, it is evident that the model predicts a much smaller C_2H_4/C_2H_6 ratio than was observed experimentally, which confirms that the oxidative dehydrogenation of C_2H_6 occurs catalytically. The model similarly underestimates the formation of C_3 products, which involves the same C_2H_5· radicals (reaction (14)) as in the conversion of C_2H_6 to C_2H_4 (reaction (13)). These radicals are formed mainly at the surface of the catalyst, a reaction that is not included in the model.

A comparable model calculation was carried out with O_2 as the oxidant. In this variation, reaction (8) was replaced by

$$O_s^{2-} + \square + \frac{1}{2}O_2 \rightarrow 2O_s^-, \qquad (15)$$

reaction (8′) was replaced by

$$O_2 \rightarrow 2O_s^-, \qquad (15')$$

and k_{15} was adjusted to obtain the CH_4 conversion reported in Table 4. Good agreement was found with $k_{15} = 2.20 \times 10^{12}\ e^{-27{,}000/T}\ s^{-1}$. At 680°C, k_{15} is approximately a factor of 14 greater than k_8. The calculated C_{2+} selectivity with 30 kPa CH_4 and 5.6 kPa O_2 was 87% at 680°C, which is much greater than the experimentally observed value of 62%. This observation supports the hypothesis that O_2 reacts with the surface to form another type of active center which is particularly nonselective. At these temperatures and pressures gas phase reactions do not serve as a major pathway for the formation of CO_2.

CONCLUSIONS

Although N_2O is an effective oxidant for the CH_4 coupling reaction, the rate of oxygen incorporation into the catalyst is slower than with O_2, which means that even at relatively small CH_4/N_2O ratios the overall reaction is limited by this step. At a given level of conversion much greater C_{2+} selectivities were observed with N_2O than with O_2. The increase in selectivity with N_2O is attributed to a decrease in CO_x forming reactions on the surface of the catalyst. The heterogeneous part of the mechanism is similar with N_2O and O_2; however, additional steps are required to account for the decomposition of N_2O and the fact that CH_4 inhibits the rate of N_2O decomposition. The poor selectivity observed with the MgO catalyst indicates that this pure oxide is intrinsically nonselective, independent of the oxidant.

ACKNOWLEDGMENT

The authors acknowledge financial support of this research by the National Science Foundation under Grant CHE-9005808.

REFERENCES

1. Otsuka, K., and Nakajima, T., *J. Chem. Soc. Faraday Trans. 1* **83,** 1315 (1987).
2. Hutchings, G. J., Scurrell, M. S., and Woodhouse, J. R., *J. Chem. Soc. Chem. Commun.*, 1388 (1987).
3. Hutchings, G. J., Scurrell, M. S., and Woodhouse, J. R., *J. Chem. Soc. Faraday Trans. 1* **85,** 2507 (1989).
4. Hutchings, G. J., and Scurrell, M. S., *in* "Methane Conversion by Oxidative Processes" (E. E. Wolf, Ed.), p. 200. Van Nostrand-Reinhold, New York, 1992.
5. Shi, C., Hatano, M., and Lunsford, J. H., *Catal. Today* **13,** 191 (1992).
6. Wong, N. B., and Lunsford, J. H., *J. Chem. Phys.* **56,** 2664 (1972).
7. Takita, Y., and Lunsford, J. H., *J. Phys. Chem.* **83,** 683 (1979).

8. Martir, W., and Lunsford, J. H., *J. Am. Chem. Soc.* **103,** 3728 (1981).
9. Dell, R. M., Stone, F. S., and Tiley, P. F., *Trans. Faraday Soc.* **49,** 201 (1953).
10. Winter, E. R. S., *J. Catal.* **15,** 144 (1969).
11. Roos, J. A., Korf, S. J., Veehof, R. H. J., Van Ommen, J. G., and Ross, J. R. H., *Appl. Catal.* **52,** 131 (1989).
12. Satterfield, C. N., "Heterogeneous Catalysis in Practice," 1st ed., p. 53. McGraw–Hill, New York, 1980.
13. Shi, C., Xu, M., Rosynek, M. P., and Lunsford, J. H., *J. Phys. Chem.* **97,** 216 (1993).
14. Lunsford, J. H., Lin, C.-H., Wang, J.-X., and Campbell, K. D., *in* "Microstructure and Properties of Catalysts" (M. M. J. Treacy, J. M. Thomas, and J. M. White, Eds.), p. 305. Materials Research Society, Pittsburgh, 1988.
15. Xu, M., Shi, C., Rosynek, M. P., and Lunsford, J. H., *J. Phys. Chem.* **96,** 6395 (1992).
16. Ito, T., Wang, J.-X., Lin, C.-H., and Lunsford, J.H., *J. Am. Chem. Soc.* **107,** 5062 (1985).
17. Iwamoto, M., and Lunsford, J. H., *Chem. Phys. Lett.* **66,** 48 (1979).
18. Westley, F., Herron, J. T., Cvetanoic, R. J., Hampson, R. F., and Mallard, G., NIST Chemical Kinetics Database, Version 3.0, National Institute of Standards and Technology, U.S. Department of Commerce, 1991.
19. Tsang, W., *J. Phys. Chem. Ref. Data.* **17,** 887 (1988).
20. Chappell, G. A., and Shaw, H., *J. Phys. Chem.* **72,** 4672 (1968).
21. Warnaatz, J., *in* "Combustion Chemistry" (W. C. Gardiner, Ed.), p. 197. Springer-Verlag, New York, 1984.
22. Allara, D. L., and Shaw, R., *J. Phys. Chem. Ref. Data.* **9,** 523 (1980).
23. Gutman, D., Lutz, R. W., Jacobs, N. F., and Hardwidge, E. A., *J. Chem. Phys.* **48,** 5689 (1968).
24. Sugawara, K., Okazaki, K., and Sato, S., *Bull. Chem. Soc. Jpn.* **54,** 2872 (1981).